impact on each BAC clone. It has been validated that screening by BAMCA, which has an ability for detecting any tendency for coordinated regulation of DNA methylation at multiple CpG sites in the entire BAC region, followed by revision using pyrosequencing, is a promising approach for carcinogenetic risk estimation. Pyrosequencing can be performed using a very small amount of degraded DNA extracted from liver biopsy specimens. In other words, unless another approach such as pyrosequencing is used to validate BAMCA data, risk assessment of liver biopsy specimens based only on BAMCA is premature. We now intend to validate the reliability of such risk estimation prospectively using liver biopsy specimens obtained prior to interferon therapy from a large cohort of patients with HBV or HCV infection.

Urothelial carcinomas are clinically remarkable because of their multicentricity owing to the 'field effect', whereby carcinogenic agents in the urine cause malignant transformation of multiple urothelial cells [66]. Even noncancerous urothelia showing no remarkable histological features obtained from patients with UCs can be considered to be at the precancerous stage, because they may be exposed to carcinogens in the urine. On the other hand, UCs are classified as superficial papillary carcinomas or nodular invasive carcinomas according to their configuration (FIGURE 4A) [66]. Superficial papillary carcinomas usually remain noninvasive, although patients need to undergo repeated urethrocystoscopic resection because of recurrences. By contrast, the clinical outcome of nodular invasive carcinoma is poor. In our previous study, accumulation of DNA methylation on C-type CpG islands associated with DNMT1 overexpression was observed even in noncancerous urothelia obtained from patients with UCs, and was further increased especially in nodular invasive carcinomas [67,68]. These previous data suggest that carcinogenetic risk estimation of UCs based on DNA methylation status might be a promising strategy.

We carefully took the tissue specimens from the surface of elevated UC lesions to avoid contamination with noncancerous urothelial and stromal cells. Principal component analysis based on BAMCA data revealed that stepwise DNA methylation alterations from 17 samples of noncancerous urothelia obtained from patients with UCs to 40 samples of UCs, in comparison with 18 samples of normal urothelia, occurred in a genome-wide manner [55]. We then performed unsupervised 2D hierarchical clustering analysis based on BAMCA data for noncancerous urothelia. The examined patients with UCs were clustered into two subclasses, clusters A_{NU} and B_{NU}. The incidence of invasive UCs (pT2 or more) was significantly higher in patients belonging to cluster B_{NU} defined on the basis of DNA methylation status in their noncancerous urothelia in comparison to cluster A_{NU} [55]. Moreover, Wilcoxon test identified the BAC clones whose signal ratios differed significantly between noncancerous urothelia obtained from patients with superficial UCs (pTa and pT1) and noncancerous urothelia obtained from patients with invasive UCs (pT2 or more). DNA methylation profiles on such BAC clones of noncancerous urothelia obtained from patients with invasive UCs were inherited by the invasive UCs themselves (FIGURE 4B) [55]. DNA methylation alterations that were correlated with the development of more malignant invasive cancers were already accumulated in noncancerous urothelia.

To estimate the degree of carcinogenetic risk based on DNA methylation profiles in noncancerous urothelia, 83 BAC clones whose signal ratios discriminated noncancerous urothelia obtained from patients with UCs from normal urothelia with a sensitivity and specificity of 75% or more than 75% were identified. We established the criteria for carcinogenetic risk estimation by combining the cutoff values of the signal ratios for these 83 BAC clones [55]. We are currently attempting to develop a methodology for assessing the tendency of DNA methylation in the 83 BAC regions in urine samples to make such risk estimation applicable to healthy individuals. If it proves possible to identify individuals who are at high risk of urothelial carcinogenesis, then strategies for the prevention or early detection of UCs, such as smoking cessation or repeated urine cytology examinations, might be applicable.

Approximately 10–30% of patients with UCs of the renal pelvis and ureter develop intravesical metachronous UCs after nephroureterectomy [69]. Therefore, such patients need to undergo repeated urethrocystoscopic examinations to detect intravesical metachronous UCs. To decrease the need for invasive urethrocystoscopic examinations and assist close follow-up of such patients after nephroureterectomy, indicators for intravesical metachronous UCs have been needed. Since such metachronous UC originates from the noncancerous urothelium of the urinary bladder, we focused on the DNA methylation status of noncancerous urothelia, which may be exposed to the same carcinogens

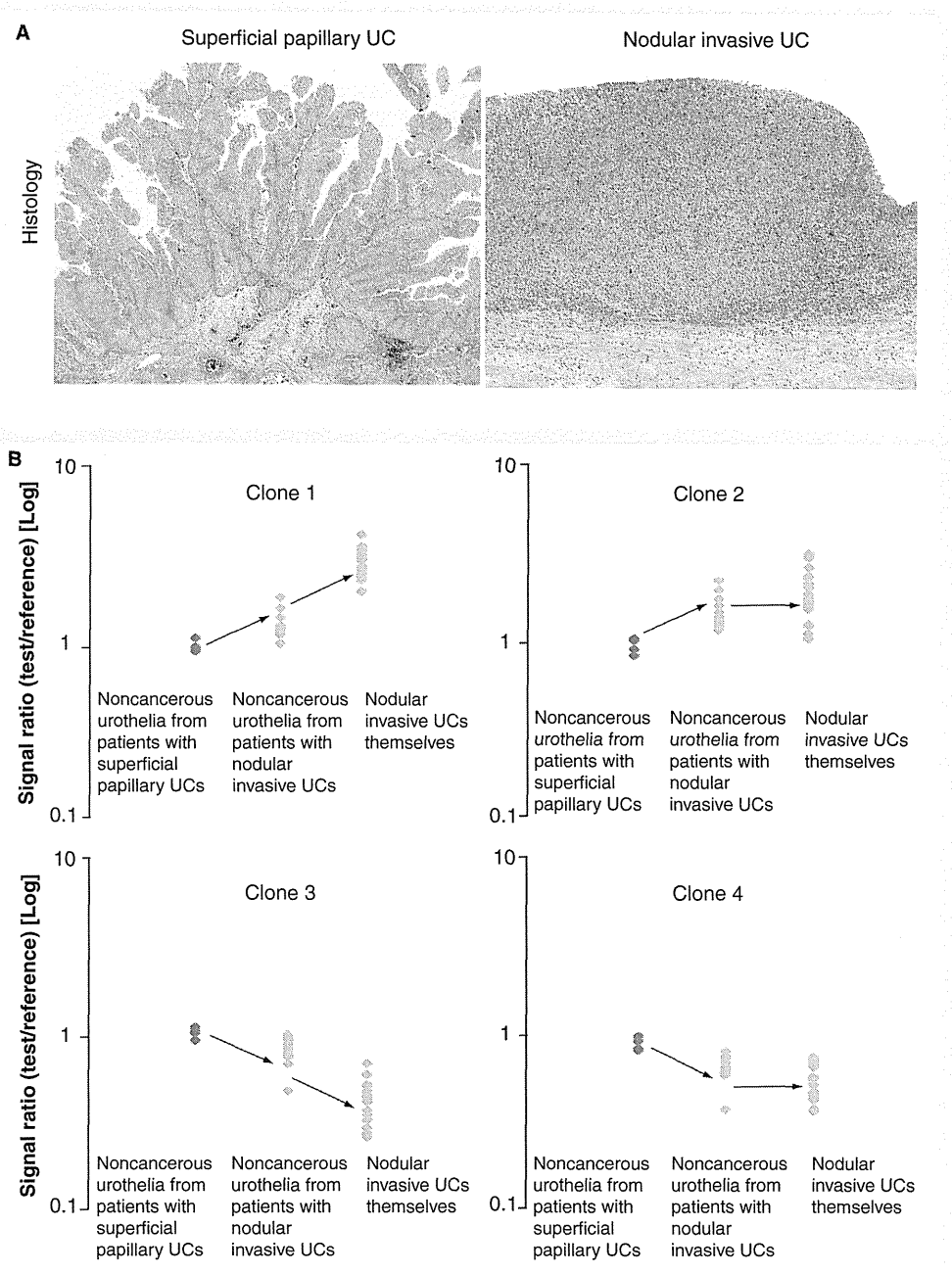

Figure 4. Significance of DNA methylation alterations at precancerous stages during urothelial carcinogenesis. For legend please see facing page.

in the urine, obtained by nephroureterectomy from patients with UCs of the renal pelvis or ureter. Unsupervised 2D hierarchical clustering analysis based on BAMCA data for noncancerous urothelia obtained from patients with UCs of the renal pelvis or ureter was able to group the examined patients into two subclasses, clusters A_{NP} and B_{NP}. The patients in cluster B_{NP} frequently developed intravesical metachronous UCs, whereas none belonging to cluster A_{NP} did so [55], indicating that DNA methylation profiles of noncancerous urothelia obtained by nephroureterectomy from patients with UCs of the renal pelvis or ureter are correlated with the risk of intravesical metachronous UC development. We identified nine BAC clones whose signal ratios discriminated noncancerous urothelia obtained from patients with UCs of the renal pelvis or ureter who developed intravesical metachronous UC after nephroureterectomy from noncancerous urothelia obtained from patients with UCs of the renal pelvis or ureter who did

Figure 4. Significance of DNA methylation alterations at precancerous stages during urothelial carcinogenesis. (A) Histological features of superficial papillary UC and nodular invasive UC. Superficial papillary carcinomas usually remain noninvasive, although patients need to undergo repeated urethrocystoscopic resection because of recurrences. By contrast, the clinical outcome of nodular invasive carcinomas is poor. **(B)** Scattergrams of the signal ratios in noncancerous urothelia obtained from patients with superficial UCs, noncancerous urothelia obtained from patients with invasive UCs, and invasive UCs themselves. Wilcoxon test revealed that the signal ratios of 131 bacterial artificial chromosome (BAC) clones differed significantly between noncancerous urothelia obtained from patients with superficial UCs and noncancerous urothelia obtained from patients with invasive UCs. If the average signal ratios in noncancerous urothelia obtained from patients with invasive UCs were significantly higher than those in noncancerous urothelia obtained from patients with superficial UCs (67 BAC clones), the average signal ratios in invasive UCs themselves were even higher than (42 BAC clones such as clone 1), or not significantly different from (25 BAC clones such as clone 2), those in noncancerous urothelia obtained from patients with invasive UCs without exception. If the average signal ratios in noncancerous urothelia obtained from patients with invasive UCs were significantly lower than those in noncancerous urothelia obtained from patients with superficial UCs (64 BAC clones), the average signal ratios in invasive UCs themselves were even lower than (38 BAC clones such as clone 3), or not significantly different from (26 BAC clones such as clone 4), those in noncancerous urothelia obtained from patients with invasive UCs without exception. Therefore, DNA methylation profiles of noncancerous urothelia obtained from patients with invasive UCs were inherited by the invasive UCs themselves.
UC: Urothelial carcinoma.

not with a sensitivity and specificity of 100% [55]. Thus, after validation using other technologies such as pyrosequencing, a combination of CpG sites on the present nine BAC clones may provide an optimal indicator for the development of intravesical metachronous UC.

Prognostication of patients with cancers based on DNA methylation profiles

Some RCCs relapse and metastasize to distant organs, even if resection has been considered complete. Recently, immunotherapy and novel targeting agents have been developed for treatment of RCC. However, unless relapsed or metastasized tumors are diagnosed early by close follow-up, the effectiveness of any therapy is very restricted. Therefore, to assist close follow-up of patients who have undergone nephrectomy and are still at risk of recurrence and metastasis, prognostic indicators have been explored. Among the examined patients in the abovementioned cluster B_{TK}, 38% died owing to recurrent RCCs, whereas only 2.3% of the patients in cluster A_{TK} died. Multivariate analysis revealed that our clustering was a predictor of recurrence and was independent of histological grade, macroscopic configuration, vascular involvement and renal vein tumor thrombi [60]. We were able to set the cutoff values of the signal ratios for 14 BAC clones to determine whether or not patients in this cohort belonged to cluster B_{TK} with a sensitivity and specificity of 100% [60].

To establish criteria for prognostication of patients with HCCs, in the learning cohort, HCC samples obtained from patients who had survived more than 4 years after hepatectomy and HCC samples obtained from patients who had suffered recurrence within 6 months and died within a year after hepatectomy were defined as a favorable-outcome group and a poor-outcome group, respectively. Wilcoxon test revealed that the signal ratios of 41 BAC clones differed significantly between the two groups (n = 19). We established the criteria for prognostication by combining the cutoff values of signal ratios for the 41 BAC clones (FIGURE 3B) [65]. Multivariate analysis revealed that satisfying the criteria for 32 or more BAC clones was a predictor of recurrence, and was independent of histological differentiation, portal vein tumor thrombi, intrahepatic metastasis and multicentricity [65]. The cancer-free and overall survival rates of patients with HCCs in the validation cohort (n = 44) satisfying the criteria for 32 or more BAC clones were significantly lower than those of patients with HCCs satisfying the criteria for less than 32 BAC clones [65]. Such prognostication using biopsy or hepatectomy specimens may be able to assist clinicians in devising therapeutic strategies for patients with insufficient liver function.

Recently, new forms of systemic chemotherapy and targeted therapy have been developed for treatment of UCs. In order to start adjuvant systemic chemotherapy immediately in patients who have undergone surgery and are still at high risk of recurrence and metastasis, prognostic indicators have been explored. It is expected that a combination of several CpG islands of tumor-related genes would be useful as epigenetic markers for prognostication of UCs [70]. In addition, when we applied BAMCA to UCs, unsupervised 2D hierarchical clustering analysis based on BAMCA data for UCs was

able to group the examined patients into two subclasses, clusters A_{TU} and B_{TU}. Among the patients belonging to cluster B_{TU}, 19% suffered recurrence after surgery, whereas none belonging to cluster A_{TU} did so [55]. Wilcoxon test revealed that the signal ratios of 20 BAC clones in UCs differed significantly between the patients who suffered recurrence after surgery and the patients who did not. The criteria for a combination of the 20 BAC clones were able to discriminate patients who suffered recurrence after surgery from patients who did not with a sensitivity and specificity of 100%, whereas a high histological grade, invasive growth (pT2 or more) and vascular or lymphatic involvement were incapable of such complete discrimination [55]. The reliability of such prognostication will need to be validated in a prospective study.

Future perspective

The incidence of DNA methylation alterations is generally high in various organs during multistage carcinogenesis. Since even subtle alterations of DNA methylation profiles at the precancerous stage are stably preserved on DNA double strands by covalent bonds, and these can be detected using highly sensitive methodology. Therefore, they may be better diagnostic indicators than mRNA and protein-expression profiles, which can be easily affected by the microenvironment of cancer cells or precursor cells. Genome-wide DNA methylation profiling can provide indicators for carcinogenetic risk estimation and prognostication using samples of urine, sputum and other body fluids, and also biopsy and surgically resected specimens. However, exploitation of diagnostic indicators can never be regarded as optimal, and it is expected that ongoing technical innovation and prospective validation will lead to further improvements of diagnostic sensitivity and specificity.

Patients with cancers are frequently clustered into subclasses showing both distinct genome-wide DNA methylation profiles and distinct clinicopathological characteristics (Figure 1B). Such clustering of cancers may provide clues for clarification of the molecular mechanisms establishing the distinct DNA methylation profiles of each cluster and the identification of target molecules for prevention and therapy in

Executive summary

Introduction

- Human cancer cells show a drastic change in DNA methylation status, that is overall DNA hypomethylation and regional DNA hypermethylation.
- DNA methylation alterations are known to result in altered expression of tumor-related genes and chromosomal instability in human cancers.

DNA methylation alterations during multistage carcinogenesis

- DNA methylation alterations play a significant role even at the precancerous stage, especially in association with chronic inflammation and persistent infection with viruses, such as hepatitis B virus or hepatitis C virus.
- DNA methyltransferase 1 overexpression in cancers is frequently correlated with accumulation of DNA methylation of tumor-related genes and poorer patient outcome.

Genome-wide DNA methylation analysis

- For genome-wide analysis, microarray platforms are used in combination with DNA methylation-sensitive restriction enzyme-based or antimethyl-cytosine antibody affinity techniques, and new generation sequencing technologies are also being introduced.
- Bacterial artificial chromosome array-based methylated CpG island amplification (BAMCA) may be suitable for overviewing the DNA methylation tendency of individual large regions among all chromosomes.

Genome-wide DNA methylation profiles at precancerous stages are inherited by cancers & determine tumor aggressiveness

- Distinct DNA methylation profiles in noncancerous tissue at the precancerous stage is basically inherited by the cancer developing in each individual patient.
- DNA methylation alterations at the precancerous stage, which may not occur randomly but may foster further epigenetic and genetic alterations, can generate more malignant cancers and even determine patient outcome.

Carcinogenetic risk estimation based on DNA methylation profiles

- On the basis of BAMCA data, criteria for estimation of the risk of hepatocellular carcinoma and urothelial carcinoma development have been established.

Prognostication of patients with cancers based on DNA methylation profiles

- On the basis of BAMCA data, criteria for the prognostication of patients with renal cell carcinomas, hepatocellular carcinomas and urothelial carcinomas have been established.

Future perspective

- Genome-wide DNA methylation profiling can provide indicators for carcinogenetic risk estimation and prognostication using samples of body fluids and tissue specimens.
- Based upon genome-wide DNA methylation profiling, translational epigenetics has come of age.

patients belonging to each cluster. Based upon of genome-wide DNA methylation profiling, translational epigenetics has clearly come of age.

Financial & competing interests disclosure

This study was supported by a Grant-in-Aid for the Third Term Comprehensive 10-Year Strategy for Cancer Control from the Ministry of Health, Labor and Welfare of Japan, a Grant-in-Aid for Cancer Research from the Ministry of Health, Labor and Welfare of Japan, a Grant from the New Energy and Industrial Technology Development Organization (NEDO), and the Program for Promotion of Fundamental Studies in Health Sciences of the National Institute of Biomedical Innovation (NiBio). The authors have no other relevant affiliations or financial involvement with any organization or entity with financial interest in or financial conflict with the subject matter or materials discussed in the manuscript apart from those disclosed.

No writing assistance was utilized in the production of this manuscript.

Ethical conduct of research

The authors state that they have obtained appropriate institutional review board approval or have followed the principles outlined in the Declaration of Helsinki for all human or animal experimental investigations. In addition, for investigations involving human subjects, informed consent has been obtained from the participants involved.

Bibliography

Papers of special note have been highlighted as:
* of interest

1 Jones PA, Baylin SB: The fundamental role of epigenetic events in cancer. *Nat. Rev. Genet.* 3, 415–428 (2002).

2 Jones PA, Baylin SB: The epigenomics of cancer. *Cell* 128, 683–692 (2007).

3 Sharma S, Kelly TK, Jones PA: Epigenetics in cancer. *Carcinogenesis* 31, 27–36 (2009).

4 Cedar H, Bergman Y: Linking DNA methylation and histone modification: patterns and paradigms. *Nat. Rev. Genet.* 10, 295–304 (2009).

5 Delcuve GP, Rastegar M, Davie JR: Epigenetic control. *J. Cell Physiol.* 219, 243–250 (2009).

6 Illingworth RS, Bird AP: CpG islands – 'a rough guide'. *FEBS Lett.* 583, 1713–1720 (2009).

7 Mohn F, Schubeler D: Genetics and epigenetics: stability and plasticity during cellular differentiation. *Trends. Genet.* 25, 129–136 (2009).

8 Yoshiura K, Kanai Y, Ochiai A, Shimoyama Y, Sugimura T, Hirohashi S: Silencing of the E-cadherin invasion-suppressor gene by CpG methylation in human carcinomas. *Proc. Natl Acad. Sci.* USA 92, 7416–7419 (1995).

* **E-cadherin tumor suppressor gene was shown to be silenced by DNA methylation, and the universality of a 'two-hit' mechanism involving DNA hypermethylation and loss of heterozygosity during carcinogenesis has been proposed.**

9 Baylin SB, Ohm JE: Epigenetic gene silencing in cancer – a mechanism for early oncogenic pathway addiction? *Nat. Rev. Cancer* 6, 107–116 (2006).

10 Shibata D: Inferring human stem cell behaviour from epigenetic drift. *J. Pathol.* 217, 199–205 (2009).

11 Ohm JE, McGarvey KM, Yu X *et al.*: A stem cell-like chromatin pattern may predispose tumor suppressor genes to DNA hypermethylation and heritable silencing. *Nat. Genet.* 39, 237–242 (2007).

12 Pogribny IP, Beland FA: DNA hypomethylation in the origin and pathogenesis of human diseases. *Cell Mol. Life Sci.* 66, 2249–2261 (2009).

13 Wong N, Lam WC, Lai PB, Pang E, Lau WY, Johnson PJ: Hypomethylation of chromosome 1 heterochromatin DNA correlates with q-arm copy gain in human hepatocellular carcinoma. *Am. J. Pathol.* 159, 465–471 (2001).

14 Nakagawa T, Kanai Y, Ushijima S, Kitamura T, Kakizoe T, Hirohashi S: DNA hypomethylation on pericentromeric satellite regions significantly correlates with loss of heterozygosity on chromosome 9 in urothelial carcinomas. *J. Urol.* 173, 243–246 (2005).

15 Okano M, Bell DW, Haber DA, Li E: DNA methyltransferases DNMT3a and Dnmt3b are essential for *de novo* methylation and mammalian development. *Cell* 99, 247–257 (1999).

16 Saito Y, Kanai Y, Sakamoto M, Saito H, Ishii H, Hirohashi S: Overexpression of a splice variant of DNA methyltransferase 3b, DNMT3b4, associated with DNA hypomethylation on pericentromeric satellite regions during human hepatocarcinogenesis. *Proc. Natl Acad. Sci. USA* 99, 10060–10065 (2002).

* **Overexpression of an inactive splice variant of DNMT3b, which competes with the major splice variant for targeting to pericentromeric satellite regions, has been proposed as one of the molecular mechanisms for chromosomal instability during hepatocarcinogenesis.**

17 Laird PW: The power and the promise of DNA methylation markers. *Nat. Rev. Cancer* 3, 253–266 (2003).

18 Issa JP, Kantarjian HM: Targeting DNA methylation. *Clin. Cancer Res.* 15, 3938–3946 (2009).

19 Swanton C, Caldas C: Molecular classification of solid tumours: towards pathway-driven therapeutics. *Br. J. Cancer* 100, 1517–1522 (2009).

20 Kanai Y, Hirohashi S: Alterations of DNA methylation associated with abnormalities of DNA methyltransferases in human cancers during transition from a precancerous to a malignant state. *Carcinogenesis* 28, 2434–2442 (2007).

* **Results of empirical analysis of DNA methylation status and DNA methyltransferase abnormalities in clinical tissue samples in connection with the clinicopathological parameters of human cancers have been reviewed.**

21 Kanai Y: Alterations of DNA methylation and clinicopathological diversity of human cancers. *Pathol. Int.* 58, 544–558 (2008).

22 Kanai Y: Genome-wide DNA methylation profiles in precancerous conditions and cancers. *Cancer Sci.* 101, 36–45 (2010).

23 Kanai Y, Ushijima S, Tsuda H, Sakamoto M, Sugimura T, Hirohashi S: Aberrant DNA methylation on chromosome 16 is an early event in hepatocarcinogenesis. *Jpn. J. Cancer Res.* 87, 1210–1217 (1996).

* **One of the earliest reports of DNA methylation alterations at the precancerous stage, especially in noncancerous liver tissue showing chronic hepatitis or cirrhosis, which are widely considered to be precancerous conditions for hepatocellular carcinomas.**

24 Kanai Y, Hui AM, Sun L *et al.*: DNA hypermethylation at the D17S5 locus and reduced HIC-1 mRNA expression are associated with hepatocarcinogenesis. *Hepatology* 29, 703–709 (1999).

25 Kondo Y, Kanai Y, Sakamoto M, Mizokami M, Ueda R, Hirohashi S: Genetic instability and aberrant DNA methylation in chronic hepatitis and cirrhosis – a comprehensive study of loss of heterozygosity and microsatellite instability at 39 loci and DNA hypermethylation on 8 CpG islands in microdissected specimens from patients with hepatocellular carcinoma. *Hepatology* 32, 970–979 (2000).

26 Etoh T, Kanai Y, Ushijima S *et al.*: Increased DNA methyltransferase 1 (DNMT1) protein expression correlates significantly with poorer tumor differentiation and frequent DNA hypermethylation of multiple CpG islands in gastric cancers. *Am. J. Pathol.* 164, 689–699 (2004).

27 Wentzensen N, Sherman ME, Schiffman M, Wang SS: Utility of methylation markers in cervical cancer early detection: appraisal of the state-of-the-science. *Gynecol. Oncol.* 112, 293–299 (2009).

28 Ushijima T: Epigenetic field for cancerization. *J. Biochem. Mol. Biol.* 40, 142–150 (2007).

29 Eguchi K, Kanai Y, Kobayashi K, Hirohashi S: DNA hypermethylation at the D17S5 locus in non-small cell lung cancers: its association with smoking history. *Cancer Res.* 57, 4913–4915 (1997).

30 Toyota M, Ahuja N, Ohe-Toyota M, Herman JG, Baylin SB, Issa JP: CpG island methylator phenotype in colorectal cancer. *Proc. Natl Acad. Sci. USA* 96, 8681–8686 (1999).

31 Kanai Y, Ushijima S, Hui AM *et al.*: The E-cadherin gene is silenced by CpG methylation in human hepatocellular carcinomas. *Int. J. Cancer* 71, 355–359 (1997).

32 Saito Y, Kanai Y, Sakamoto M, Saito H, Ishii H, Hirohashi S: Expression of mRNA for DNA methyltransferases and methyl-CpG-binding proteins and DNA methylation status on CpG islands and pericentromeric satellite regions during human hepatocarcinogenesis. *Hepatology* 33, 561–568 (2001).

33 Saito Y, Kanai Y, Nakagawa T *et al.*: Increased protein expression of DNA methyltransferase (DNMT) 1 is significantly correlated with the malignant potential and poor prognosis of human hepatocellular carcinomas. *Int. J. Cancer* 105, 527–532 (2003).

34 Peng DF, Kanai Y, Sawada M *et al.*: Increased DNA methyltransferase 1 (DNMT1) protein expression in precancerous conditions and ductal carcinomas of the pancreas. *Cancer Sci.* 96, 403–408 (2005).

35 Peng DF, Kanai Y, Sawada M *et al.*: DNA methylation of multiple tumor-related genes in association with overexpression of DNA methyltransferase 1 (DNMT1) during multistage carcinogenesis of the pancreas. *Carcinogenesis* 27, 1160–1168 (2006).

36 Ooi SK, O'Donnell AH, Bestor TH: Mammalian cytosine methylation at a glance. *J. Cell Sci.* 122, 2787–2791 (2009).

37 Chuang LS, Ian HI, Koh TW, Ng HH, Xu G, Li BF: Human DNA-(cytosine-5) methyltransferase-PCNA complex as a target for p21WAF1. *Science* 277, 1996–2000 (1997).

38 Kanai Y, Ushijima S, Kondo Y, Nakanishi Y, Hirohashi S: DNA methyltransferase expression and DNA methylation of CpG islands and peri-centromeric satellite regions in human colorectal and stomach cancers. *Int. J. Cancer* 91, 205–212 (2001).

39 Damiani LA, Yingling CM, Leng S, Romo PE, Nakamura J, Belinsky SA: Carcinogen-induced gene promoter hypermethylation is mediated by DNMT1 and causal for transformation of immortalized bronchial epithelial cells. *Cancer Res.* 68, 9005–9014 (2008).

40 Liao X, Siu MK, Chan KY *et al.*: Hypermethylation of RAS effector related genes and DNA methyltransferase 1 expression in endometrial carcinogenesis. *Int. J. Cancer* 123, 296–302 (2008).

41 Hino R, Uozaki H, Murakami N *et al.*: Activation of DNA methyltransferase 1 by EBV latent membrane protein 2A leads to promoter hypermethylation of *PTEN* gene in gastric carcinoma. *Cancer Res.* 69, 2766–2774 (2009).

42 Gao P, Yang X, Xue YW *et al.*: Promoter methylation of glutathione *S*-transferase pi1 and multidrug resistance gene 1 in bronchioloalveolar carcinoma and its correlation with DNA methyltransferase 1 expression. *Cancer* 115, 3222–3232 (2009).

43 Lin RK, Hsieh YS, Lin P *et al.*: The tobacco-specific carcinogen NNK induces DNA methyltransferase 1 accumulation and tumor suppressor gene hypermethylation in mice and lung cancer patients. *J. Clin. Invest.* 120, 521–532 (2010).

44 Eads CA, Danenberg KD, Kawakami K, Saltz LB, Danenberg PV, Laird PW: CpG island hypermethylation in human colorectal tumors is not associated with DNA methyltransferase overexpression. *Cancer Res.* 59, 2302–2306 (1999).

45 Park HJ, Yu E, Shim YH: DNA methyltransferase expression and DNA hypermethylation in human hepatocellular carcinoma. *Cancer Lett.* 233, 271–278 (2006).

46 Kondo Y, Shen L, Suzuki S *et al.*: Alterations of DNA methylation and histone modifications contribute to gene silencing in hepatocellular carcinomas. *Hepatol. Res.* 37, 974–983 (2007).

47 Estecio MR, Yan PS, Ibrahim AE *et al.*: High-throughput methylation profiling by MCA coupled to CpG island microarray. *Genome Res.* 17, 1529–1536 (2007).

48 Estecio MR, Issa JP: Tackling the methylome: recent methodological advances in genome-wide methylation profiling. *Genome Med.* 1, 106 (2009).

49 Bibikova M, Fan JB: GoldenGate assay for DNA methylation profiling. *Methods Mol. Biol.* 507, 149–163 (2009).

50 Gunderson KL: Whole-genome genotyping on bead arrays. *Methods Mol. Biol.* 529, 197–213 (2009).

51 Eid J, Fehr A, Gray J *et al.*: Real-time DNA sequencing from single polymerase molecules. *Science* 323, 133–138 (2009).

52 Maekita T, Nakazawa K, Mihara M *et al.*: High levels of aberrant DNA methylation in *Helicobacter pylori*-infected gastric mucosae and its possible association with gastric cancer risk. *Clin. Cancer Res.* 12, 989–995 (2006).

53 Clark SJ: Action at a distance: epigenetic silencing of large chromosomal regions in carcinogenesis. *Hum. Mol. Genet.* 16(Spec. No. 1), R88–R95 (2007).

54 Inazawa J, Inoue J, Imoto I: Comparative genomic hybridization (CGH)-arrays pave the way for identification of novel cancer-related genes. *Cancer Sci.* 95, 559–563 (2004).

55 Nishiyama N, Arai E, Chihara Y *et al.*: Genome-wide DNA methylation profiles in urothelial carcinomas and urothelia at the precancerous stage. *Cancer Sci.* 101, 231–240 (2010).

* **Indicators for risk estimation of the development of urothelial carcinomas and prognostication of patients with urothelial carcinomas have been established based on bacterial artificial chromosome array-based methylated CpG island amplification (BAMCA) data.**

56 Misawa A, Inoue J, Sugino Y *et al.*: Methylation-associated silencing of the nuclear receptor *1I2* gene in advanced-type neuroblastomas, identified by bacterial artificial chromosome array-based methylated CpG island amplification. *Cancer Res.* 65, 10233–10242 (2005).

57 Tanaka K, Imoto I, Inoue J *et al.*: Frequent methylation-associated silencing of a candidate tumor-suppressor, CRABP1, in esophageal squamous-cell carcinoma. *Oncogene* 26, 6456–6468 (2007).

58 Sugino Y, Misawa A, Inoue J *et al.*: Epigenetic silencing of prostaglandin E receptor 2 (PTGER2) is associated with progression of neuroblastomas. *Oncogene* 26, 7401–7413 (2007).

59 McRonald FE, Morris MR, Gentle D *et al.*: CpG methylation profiling in VHL related and VHL unrelated renal cell carcinoma. *Mol. Cancer* 8, 31–41 (2009).

60 Arai E, Ushijima S, Fujimoto H *et al.*: Genome-wide DNA methylation profiles in both precancerous conditions and clear cell renal cell carcinomas are correlated with malignant potential and patient outcome. *Carcinogenesis* 30, 214–221 (2009).

* **Genome-wide DNA methylation profiles in precancerous conditions of the kidney have been shown to be inherited by clear cell renal cell carcinomas developing in each individual patient, and to determine tumor aggressiveness and patient outcome.**

61 Arai E, Kanai Y, Ushijima S, Fujimoto H, Mukai K, Hirohashi S: Regional DNA hypermethylation and DNA methyltransferase (DNMT) 1 protein overexpression in both renal tumors and corresponding nontumorous renal tissues. *Int. J. Cancer* 119, 288–296 (2006).

62 Arai E, Ushijima S, Tsuda H *et al.*: Genetic clustering of clear cell renal cell carcinoma based on array-comparative genomic hybridization: its association with DNA methylation alteration and patient outcome. *Clin. Cancer Res.* 14, 5531–5539 (2008).

63 Lee HS, Kim BH, Cho NY *et al.*: Prognostic implications of and relationship between CpG island hypermethylation and repetitive DNA hypomethylation in hepatocellular carcinoma. *Clin. Cancer Res.* 15, 812–820 (2009).

64 Moribe T, Iizuka N, Miura T *et al.*: Methylation of multiple genes as molecular markers for diagnosis of a small, well-differentiated hepatocellular carcinoma. *Int. J. Cancer* 125, 388–397 (2009).

65 Arai E, Ushijima S, Gotoh M *et al.*: Genome-wide DNA methylation profiles in liver tissue at the precancerous stage and in hepatocellular carcinoma. *Int. J. Cancer* 125, 2854–2862 (2009).

* **Indicators for carcinogenetic risk estimation in chronically diseased liver, and prognostication of patients with hepatocellular carcinomas, have been established based on BAMCA data.**

66 Kakizoe T: Development and progression of urothelial carcinoma. *Cancer Sci.* 97, 821–828 (2006).

67 Nakagawa T, Kanai Y, Ushijima S, Kitamura T, Kakizoe T, Hirohashi S: DNA hypermethylation on multiple CpG islands associated with increased DNA methyltransferase DNMT1 protein expression during multistage urothelial carcinogenesis. *J. Urol.* 173, 1767–1771 (2005).

68 Nakagawa T, Kanai Y, Saito Y, Kitamura T, Kakizoe T, Hirohashi S: Increased DNA methyltransferase 1 protein expression in human transitional cell carcinoma of the bladder. *J. Urol.* 170, 2463–2466 (2003).

69 Manabe D, Saika T, Ebara S *et al.*: Comparative study of oncologic outcome of laparoscopic nephroureterectomy and standard nephroureterectomy for upper urinary tract transitional cell carcinoma. *Urology* 69, 457–461 (2007).

70 Kim WJ, Kim YJ: Epigenetic markers as promising prognosticators for bladder cancer. *Int. J. Urol.* 16, 17–22 (2009).

UICC
global cancer control

IJC
International Journal of Cancer

Carcinogenetic risk estimation based on quantification of DNA methylation levels in liver tissue at the precancerous stage

Ryo Nagashio[1], Eri Arai[1], Hidenori Ojima[1], Tomoo Kosuge[2], Yutaka Kondo[3] and Yae Kanai[1]

[1] Pathology Division, National Cancer Center Research Institute, Tokyo, Japan
[2] Hepatobiliary and Pancreatic Surgery Division, National Cancer Center Hospital, Tokyo, Japan
[3] Division of Molecular Oncology, Aichi Cancer Center Research Institute, Nagoya, Japan

For appropriate surveillance of patients at the precancerous stage for hepatocellular carcinomas (HCCs), carcinogenetic risk estimation is advantageous. The aim of our study was to establish criteria for such estimation based on DNA methylation profiling. The DNA methylation status of 203 CpG sites on 25 bacterial artificial chromosome (BAC) clones, whose DNA methylation status had been proven to discriminate samples of noncancerous liver tissue obtained from patients with HCC (N) from normal liver tissue (C) samples by BAC array-based methylated CpG island amplification, was evaluated quantitatively using pyrosequencing. The 45 CpG sites whose DNA methylation levels differed significantly between C and N in the learning cohort (n = 22) were identified. The criteria combining DNA methylation status for the 30 regions including the 45 CpG sites were able to diagnose N as being at high risk of carcinogenesis with 100% sensitivity and specificity in the learning cohort and 95.6% sensitivity and 100% specificity in the validation (n = 90) cohort. DNA methylation status for the 30 regions in N samples was significantly correlated with the outcome of patients with HCCs, indicating that clinicopathologically valid DNA methylation alterations have already accumulated at the precancerous stage. The DNA methylation status of the 30 regions did not depend on the presence or absence of hepatitis virus infection, or the status of noncancerous liver tissue (chronic hepatitis or cirrhosis). These criteria may be applicable for carcinogenetic risk estimation using liver biopsy specimens obtained from patients who are followed up because of chronic liver diseases.

Early Detection and Diagnosis

Hepatocellular carcinoma (HCC) is a common malignancy worldwide. Hepatitis virus infection is associated with an extremely high risk of HCC development. Although mass vaccination against hepatitis B virus (HBV) has been initiated, HBV-associated liver carcinogenesis will not be stamped out for many years, as the age at presentation of HBV is over 50 years mainly in Asia and Africa.[1] The spread of hepatitis C virus (HCV) in Japan that occurred in the 1950s and 1960s has resulted in a rapid increase in the incidence of HCC since 1980s.[2] In other countries, including the United States, HCV infection has spread more recently.[2] As HCC usually develops in liver already affected by chronic hepatitis or liver cirrhosis associated with hepatitis virus infection, the prognosis of patients with HCC is deemed poor, unless the cancer is diagnosed at an early stage. Therefore, surveillance at the precancerous stage will become a priority. In clinical practice, especially intensive surveillance should be performed on patients at high risk of HCC development, even if the patients are asymptomatic. Thus, risk estimation for HCC development is essential for the management of patients with chronic liver diseases.

Alterations of DNA methylation are among the most consistent epigenetic changes observed during multistage human carcinogenesis.[3,4] Accumulating evidence suggests that alterations of DNA methylation are involved even in the early and precancerous stages.[5,6] With respect to hepatocarcinogenesis, DNA methylation alterations associated with expression and/or splicing abnormalities of DNA methyltransferases are already present in liver tissues exhibiting chronic hepatitis or liver cirrhosis obtained from patients with HCCs.[7–11] Differing from alterations of mRNA and protein expression, which can be easily affected by the microenvironment of cancer

Key words: chronic hepatitis, hepatocellular carcinoma, liver cirrhosis, precancerous condition, pyrosequencing

Abbreviations: anti-HCV: anti-HCV antibody; BAC: bacterial artificial chromosome; BAMCA: BAC array-based methylated CpG island amplification; HBs-Ag: HBV surface antigen; HBV: hepatitis B virus; HCC: hepatocellular carcinoma; HCV: hepatitis C virus; PCR: polymerase chain reaction

Additional Supporting Information may be found in the online version of this article.

Grant sponsors: Third Term Comprehensive 10-Year Strategy for Cancer Control from the Ministry of Health, Labor and Welfare of Japan, Cancer Research from the Ministry of Health, Labor and Welfare of Japan, Program for Promotion of Fundamental Studies in Health Sciences of the National Institute of Biomedical Innovation (NiBio), Foundation for Promotion of Cancer Research in Japan

DOI: 10.1002/ijc.26061

History: Received 7 Oct 2010; Accepted 17 Feb 2011; Online 11 Mar 2011

Correspondence to: Yae Kanai, Pathology Division, National Cancer Center Research Institute, 5-1-1 Tsukiji, Chuo-ku, Tokyo 104-0045, Japan, Tel.: +81-3-3542-2511, Fax: +81-3-3248-2463, E-mail: ykanai@ncc.go.jp

cells or precursor cells, DNA methylation alterations are stably preserved on DNA double strands by covalent bonds. Therefore, even subtle alterations at the precancerous stage can be detected using highly sensitive methodology. DNA methylation alterations may be optimal indicators for carcinogenetic risk estimation.[12,13]

We have already established criteria for estimation of the risk of HCC development using bacterial artificial chromosome (BAC) array-based methylated CpG island amplification (BAMCA),[14–19] which can provide an overview of the DNA methylation tendency of individual large regions among all chromosomes;[13,19] 25 BAC clones, whose DNA methylation status was able to discriminate noncancerous liver tissue obtained from patients with HCCs in the learning cohort from normal liver tissue obtained from patients without HCCs, were identified.[18] However, sensitivity and specificity of such discrimination were not 100% in the validation cohort. Moreover, the CpG sites that are of diagnostic importance are unclear on each of the BAC clones with an average insert size of 170 kbp.[20] As the technique of BAMCA requires a large amount of genomic DNA and is somewhat cumbersome, risk estimation using BAMCA may be difficult to apply in a clinical setting.

Here, to identify precisely the CpG sites having the largest diagnostic impact, we quantitatively evaluated the DNA methylation status of 203 CpG sites on these 25 BAC clones using pyrosequencing in tissue specimens. Among the CpG sites, we were able to improve the specificity of carcinogenetic risk estimation by combining those showing the largest diagnostic impact and to apply such risk estimation to a very small amount of genomic DNA with a view to clinical application.

Material and Methods

Patients and tissue samples

As a learning cohort, 10 samples of normal liver tissue (C1–C10) showing no remarkable histological findings were obtained from specimens surgically resected from 10 patients without HCCs who were negative for both HBV surface antigen (HBs-Ag) and anti-HCV antibody (anti-HCV). The patients comprised seven men and three women with a mean (± standard deviation) age of 58.4 ± 9.7 years. Nine patients underwent partial hepatectomy for liver metastases of primary colon cancer, and one patient did so for liver metastases of a gastrointestinal stromal tumor of the stomach at the National Cancer Center Hospital, Tokyo, Japan. A total of 12 samples of noncancerous liver tissue (N1–N12) were obtained from 12 patients who underwent partial hepatectomy for HCCs. These patients comprised nine men and three women with a mean age of 65.3 ± 6.4 years. Among them, six were positive for HBs-Ag and six were positive for anti-HCV. Histological examination of these noncancerous liver tissue samples revealed findings compatible with chronic hepatitis in four and cirrhosis in eight.

As a validation cohort, 45 samples of normal liver tissue (C11–C55) exhibiting no remarkable histological findings were obtained from 45 patients without HCCs who were negative for both HBs-Ag and anti-HCV. The patients comprised 34 men and 11 women with a mean age of 62.2 ± 7.0 years. A total of 39 patients underwent partial hepatectomy for liver metastases from primary colon cancer, three patients did so for liver metastasis from gastric cancer and the remaining three patients did so for liver metastasis from each of gastrointestinal stromal tumor of the stomach, pancreatic cancer and colon carcinoid tumor, respectively. A total of 45 samples of noncancerous liver tissue (N13–N57) were obtained from 45 patients who underwent partial hepatectomy for HCCs. The patients comprised 37 men and eight women with a mean age of 62.3 ± 9.7 years. Of them 13 were positive for HBs-Ag, 29 were positive for anti-HCV, and three were negative for both. Histological examination of these noncancerous liver tissue samples revealed findings compatible with chronic hepatitis in 22 and cirrhosis in 23.

For comparison, 34 samples of primary HCC (T1–T34) were also obtained from specimens surgically resected from the patients who had provided the samples N1–N34. In addition, for comparison, 14 samples of liver tissue (V1–V14) were obtained from 14 patients who were positive for HBs-Ag or anti-HCV, but who had never developed HCCs. The patients comprised six men and eight women with a mean age of 65.1 ± 8.2 years. Of them, 12 patients underwent partial hepatectomy for liver metastases of primary colorectal cancer and two patients did so for liver metastases of gastric cancer.

Our study was approved by the Ethics Committee of the National Cancer Center, Tokyo, Japan. All the patients gave informed consent before their inclusion in our study.

DNA extraction and bisulfite DNA modification

High-molecular-weight DNA from fresh-frozen tissue samples was extracted using phenol–chloroform followed by dialysis. Bisulfite conversion was carried out using 1 μg of genomic DNA and the reagents provided in the EpiTect Bisulfite Kit (QIAGEN GmbH, Hilden, Germany), in accordance with the manufacturer's protocol. This process converts unmethylated cytosine residues to uracil, whereas methylated cytosine residues remain unchanged.[21]

Pyrosequencing DNA methylation analysis

DNA methylation level was measured by a highly quantitative method using Pyrosequencing™ technology. Polymerase chain reaction (PCR) and sequencing primers were designed based on the converted sequences using Pyrosequencing Assay Design Software ver.1.0 (QIAGEN GmbH). To overcome PCR bias in DNA methylation analysis, we optimized the annealing temperature as described previously.[22,23] Each of the primer sequences and PCR conditions are given in Supporting Information Table 1. The PCR was carried out with 0.6 units of AmpliTaq Gold (Applied Biosystems, Foster City, CA) using 7.5 ng of bisulfite-treated DNA. The

Table 1. Thirty regions that were able to discriminate noncancerous liver tissues (N) from normal liver tissues (C)

Region	BAC clone ID	Location	Characteristics	Gene	Cutoff value (%)	DNA methylation status[1]	Sensitivity (%)	Specificity (%)
1	RP11–104J13	1p35.2	Noncoding/CpG island	None	25.5	C > N	80.0	66.7
2	RP11–104J13	1p35.2	Noncoding	None	26.0	C > N	90.0	91.7
3	RP11–104J13	1p35.2	First intron/CpG island	SDC3	34.0	C > N	90.0	91.7
4	RP11–104J13	1p35.2	Noncoding	None	88.9	C < N	100	66.7
5	RP11–52I2	1p33	First exon/CpG island	FOXD2	47.5	C > N	90.0	91.7
6	RP11–29M22	1p12	Intron	PHGDH	73.0	C < N	100	50.0
7	RP11–21K1	2q37.1	Noncoding	None	93.0	C > N	80.0	50.0
8	RP11–109B15	5q33.1	Noncoding	None	12.0	C < N	80.0	83.3
9	RP11–112B7	7p13	First intron/CpG island	CAMK2B	45.0	C > N	20.0	91.7
10	RP11–120E20	11p15.4	Intron	ART5	85.0	C > N	50.0	100
11	RP11–120E20	11p15.4	Intron/SINE repeat	NUP98	95.7	C < N	100	75.0
12	RP11–334E6	11q23.3	First exon/CpG island	C1QTNF5	23.7	C < N	100	25.0
13	RP11–334E6	11q23.3	First intron/CpG island	THY1	12.6	C > N	60.0	83.3
14	RP11–17M17	11q25	First intron	OPCML	74.0	C > N	100	91.7
15	RP11–17M17	11q25	First intron	OPCML	79.0	C > N	100	33.3
16	RP11–17M17	11q25	First intron	OPCML	49.7	C > N	70.0	50.0
17	RP11–319E16	12p13.32	Noncoding	None	79.0	C > N	70.0	58.3
18	RP11–319E16	12p13.32	Noncoding/SINE repeat	None	45.0	C > N	100	50.0
19	RP11–1100L3	12q13.13	UTR	ACVRL1	50.0	C < N	90.0	83.3
20	RP11–1100L3	12q13.13	Promoter/CpG island	GRASP	7.0	C > N	80.0	58.3
21	RP11–799O6	12q13.3	UTR	ZBTB39	40.0	C < N	100	91.7
22	RP11–799O6	12q13.3	Noncoding/SINE repeat	None	89.0	C < N	80.0	100
23	RP11–89M4	16p13.3	Noncoding	None	38.0	C < N	70.0	100
24	RP11–89M4	16p13.3	Intron	LOC342346	69.0	C > N	100	33.3
25	RP11–89M4	16p13.3	Exon/CpG island	MGRN1	51.0	C < N	100	100
26	RP11–89M4	16p13.3	Intron	MGRN1	28.0	C < N	100	50.0
27	RP11–89M4	16p13.3	Intron/CpG island	MGRN1	67.0	C < N	100	100
28	RP11–348B12	19p13.3	Intron/CpG island	KDM4B	44.0	C < N	100	100
29	RP11–348B12	19p13.3	Intron/CpG island	KDM4B	94.8	C < N	100	41.7
30	RP11–348B12	19p13.3	Intron/CpG island	KDM4B	94.0	C > N	50.0	91.7

[1]C > N, when the signal ratio was lower than the cutoff value, the tissue sample was considered to be at high risk for carcinogenesis; C < N, when the signal ratio was higher than the cutoff value, the tissue sample was considered to be at high risk for carcinogenesis.

biotinylated PCR product was captured on streptavidin-coated beads (Streptavidin Sepharose™ High Performance; GE Healthcare, Uppsala, Sweden). Quantitative sequencing was run on the PyroMark Q24 (QIAGEN GmbH) using the Pyro Gold Reagents (QIAGEN GmbH) in accordance with the manufacturer's protocol. For each assay, the setup included positive controls (Epitect methylated human control DNA; QIAGEN GmbH) and negative controls (Epitect unmethylated human control DNA; QIAGEN GmbH). The PCR products were separated electrophoretically on 3% agarose gel and stained with ethidium bromide to confirm that specific products of the appropriate size and no nonspecific products were obtained on amplification. Representative pyrograms are shown in Figure 1.

As outlined in Figure 1, the DNA methylation level (%) at each CpG site is given by the following formula:

$$\text{luminescence strength of cytosine} / (\text{luminescence strength of cytosine} + \text{luminescence strength of thymine}) \times 100.$$

Statistics

Significant differences in DNA methylation levels at each of the CpG sites between groups of samples were analyzed using the Mann-Whitney *U* test. Survival curves of patient groups with HCCs were calculated by the Kaplan–Meier method,

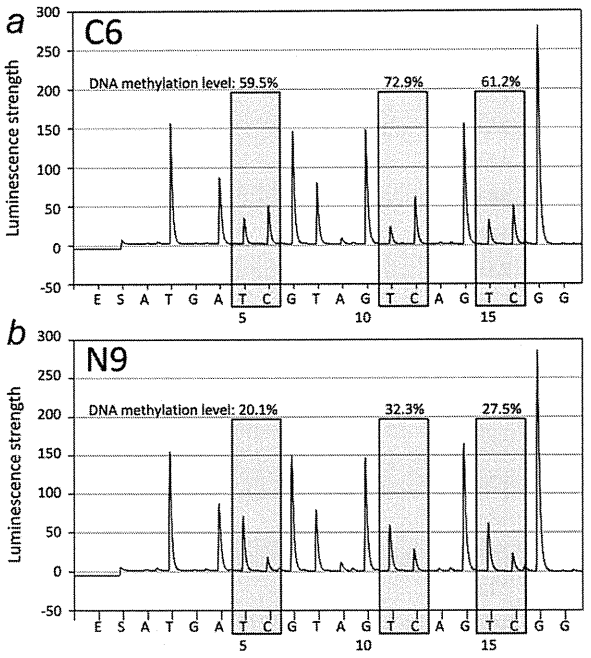

Figure 1. Pyrosequencing DNA methylation analysis. Examples of pyrograms for a sample of normal liver tissue obtained from a patient without HCC (C6) and a sample of noncancerous liver tissue obtained from a patient with HCC (N9) for exon 1 of the *FOXD2* gene (47,677,654, −60, −63 in region 5 in Table 1). Gray columns represent the regions of polymorphic sites after bisulfite modification. *x*-axis indicates dispensation order (time).

and the differences were compared by log-rank test. Differences at $p < 0.05$ were considered significant.

Results

Validation of BAMCA data by pyrosequencing

It has been shown that BAMCA can provide an overview of the DNA methylation tendency of individual large regions among all chromosomes.[13,19] Therefore, using pyrosequencing, we evaluated the DNA methylation levels of all *Xma* I/*Sma* I sites, which yielded less than 2,000 bp PCR products that are effective in BAMCA, on representative BAC clones, which had been identified as indicators for carcinogenetic risk estimation in our previous study.[18] For example, on clone RP11-17M17, there were 10 *Xma* I/*Sma* I sites that were effective in BAMCA (Fig. 2*a*). The average signal ratio by BAMCA of this BAC clone was significantly lower in samples of noncancerous liver tissue obtained from patients with HCCs than in samples of normal liver tissue and was significantly lower in HCCs than in samples of noncancerous liver tissue obtained from patients with HCCs in our previous study.[18] The average DNA methylation levels determined by pyrosequencing of all 10 *Xma* I/*Sma* I sites on this BAC clone in 34 samples of noncancerous liver tissue obtained from patients with HCCs were the same as (*Xma* I/*Sma* I sites i, ii, vii, viii and ix in Fig. 2*a*) or significantly lower than (iii, iv, v, vi and x in Fig. 2*a*) those in 35 samples of normal liver tissue. Moreover, the DNA methylation levels of all *Xma* I/*Sma* I sites in 34 HCCs were significantly lower than those in samples of noncancerous liver tissue obtained from patients with HCCs (i–x in Fig. 2*a*). DNA methylation levels of CpG sites adjacent to the *Xma* I/*Sma* I sites that were quantitatively sequenced using the same sequencing primers tended to be close to the DNA methylation levels of the *Xma* I/*Sma* I sites themselves in each sample, such as iii and iii′ and iv and iv′ in Figure 2*b*. Thus, it was confirmed that BAMCA was able to successfully reveal DNA methylation alterations occurring in a coordinated manner on RP11-17M17. In another BAC clone, RP11-799O6, which was also identified as an indicator for carcinogenetic risk estimation, the average signal ratio obtained by BAMCA was significantly higher in samples of noncancerous liver tissue from patients with HCCs than in samples of normal liver tissue in our previous study.[18] Although the average DNA methylation levels of seven out of 10 *Xma* I/*Sma* I sites, which yielded PCR products of less than 2,000 bp that are effective for BAMCA, by pyrosequencing in samples of noncancerous liver tissue from patients with HCCs were the same as those in samples of normal liver tissue, those of the remaining three *Xma* I/*Sma* I sites in samples of noncancerous liver tissue obtained from patients with HCCs were markedly higher than those in samples of normal liver tissue (data not shown). Thus, pyrosequencing data again validated the BAMCA data for BAC clones identified as indicators for carcinogenetic risk estimation.

Criteria for carcinogenetic risk estimation using liver tissue samples based on pyrosequencing

To identify CpG sites having the largest diagnostic impact, DNA methylation levels of 203 CpG sites were measured by pyrosequencing using primer sets encompassing *Xma* I/*Sma* I sites, which were effective in BAMCA, on the 25 BAC clones on which we based our previous criteria.[18]

On 59 CpG sites, the average DNA methylation levels differed significantly between normal liver tissue and noncancerous liver tissue obtained from patients with HCCs in the learning cohort using Mann-Whitney *U* test ($p < 0.001$). To establish reproducible criteria, 14 CpG sites whose average DNA methylation levels in both normal liver tissue and noncancerous liver tissue obtained from patients with HCCs were less than 10% were omitted from the list of candidate indicators for carcinogenetic risk estimation, taking the characteristics of Pyrosequencing™ technology into consideration.[22] Figure 3*a* shows scattergrams of the DNA methylation levels in samples of normal liver tissue and noncancerous liver tissue obtained from patients with HCCs on representative CpG sites. Using the cutoff values described in each panel, noncancerous liver tissue obtained from patients with

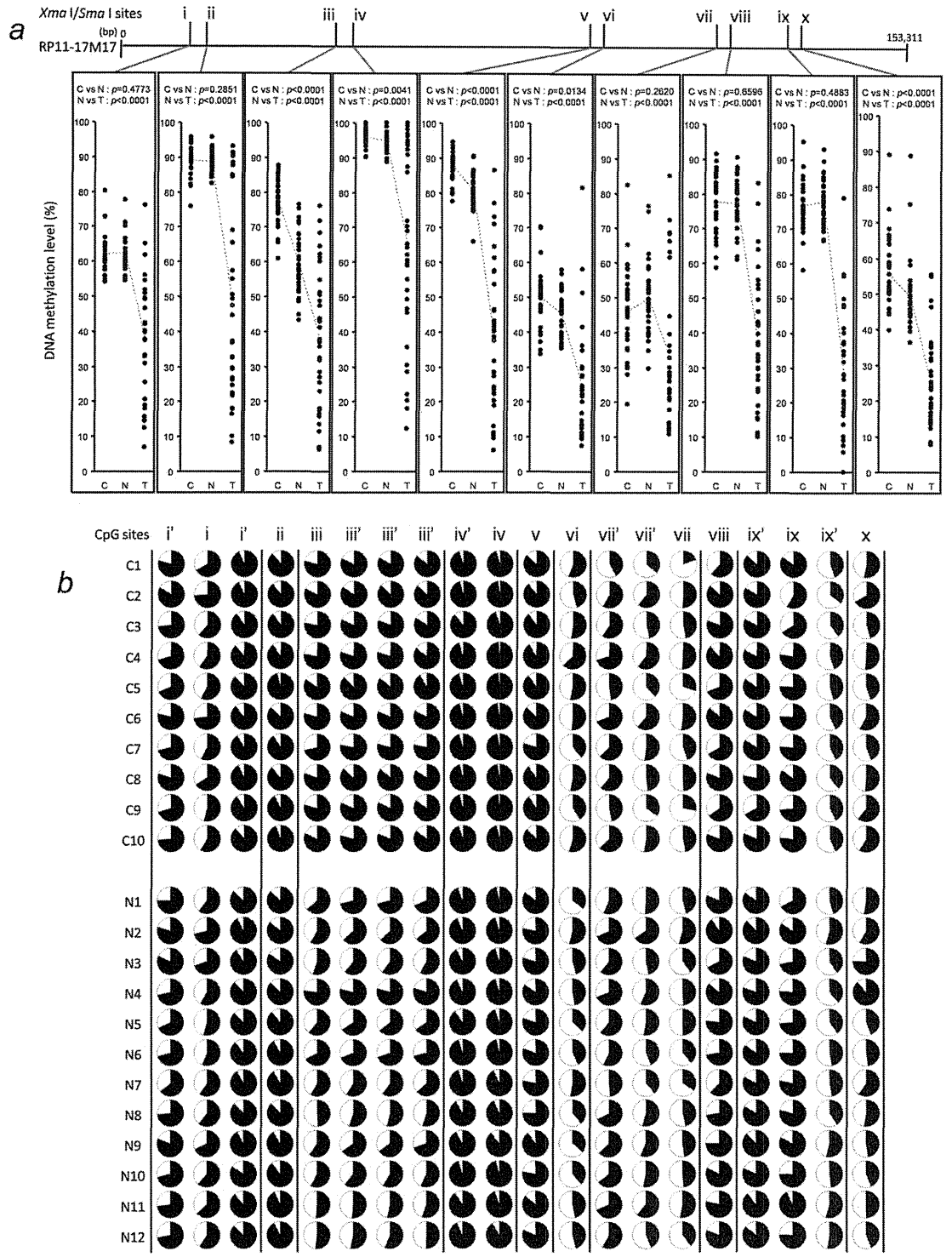

Figure 2. Validation of BAMCA data by pyrosequencing. On RP11-17M17 clone, there were 10 *Xma* I/*Sma* I sites (i–x) that yielded PCR products of less than 2,000 bp that were effective in BAMCA. The average signal ratio obtained by BAMCA for this BAC clone was significantly lower in samples of noncancerous liver tissue obtained from patients with HCCs (N) than in those of normal liver tissue (C) and was significantly lower in HCCs than in N-samples.[18] (*a*) Scattergrams of DNA methylation levels analyzed by pyrosequencing in C-samples (C1–C35), N-samples (N1–N34) and HCCs (T1–T34) on each *Xma* I/*Sma* I site. The average DNA methylation levels obtained by pyrosequencing for all 10 *Xma* I/*Sma* I sites on this BAC clone in 34 N-samples were the same as (on i, ii, vii, viii and ix) or significantly lower than (on iii, iv, v, vi and x) those in 35 C-samples. Moreover, DNA methylation levels in 34 HCCs were significantly lower than those in N-samples (on i–x). (*b*) Pi-charts of DNA methylation levels in C-samples (C1–C10) and N-samples (N1–N12) for each of the CpG sites. CpG sites adjacent to the *Xma* I/*Sma* I site (i, iii, iv, vii and ix), which were quantitatively sequenced using the same sequencing primers, are indicated by i′, iii′, iv′, vii′ and ix′, respectively. White indicates unmethylated cytosine and black indicates methylated cytosine. DNA methylation levels of CpG sites adjacent to the *Xma* I/*Sma* I sites tend to be close to the DNA methylation levels of the *Xma* I/*Sma* I sites themselves, *e.g.*, iii and iii′ and iv and iv′, in each sample.

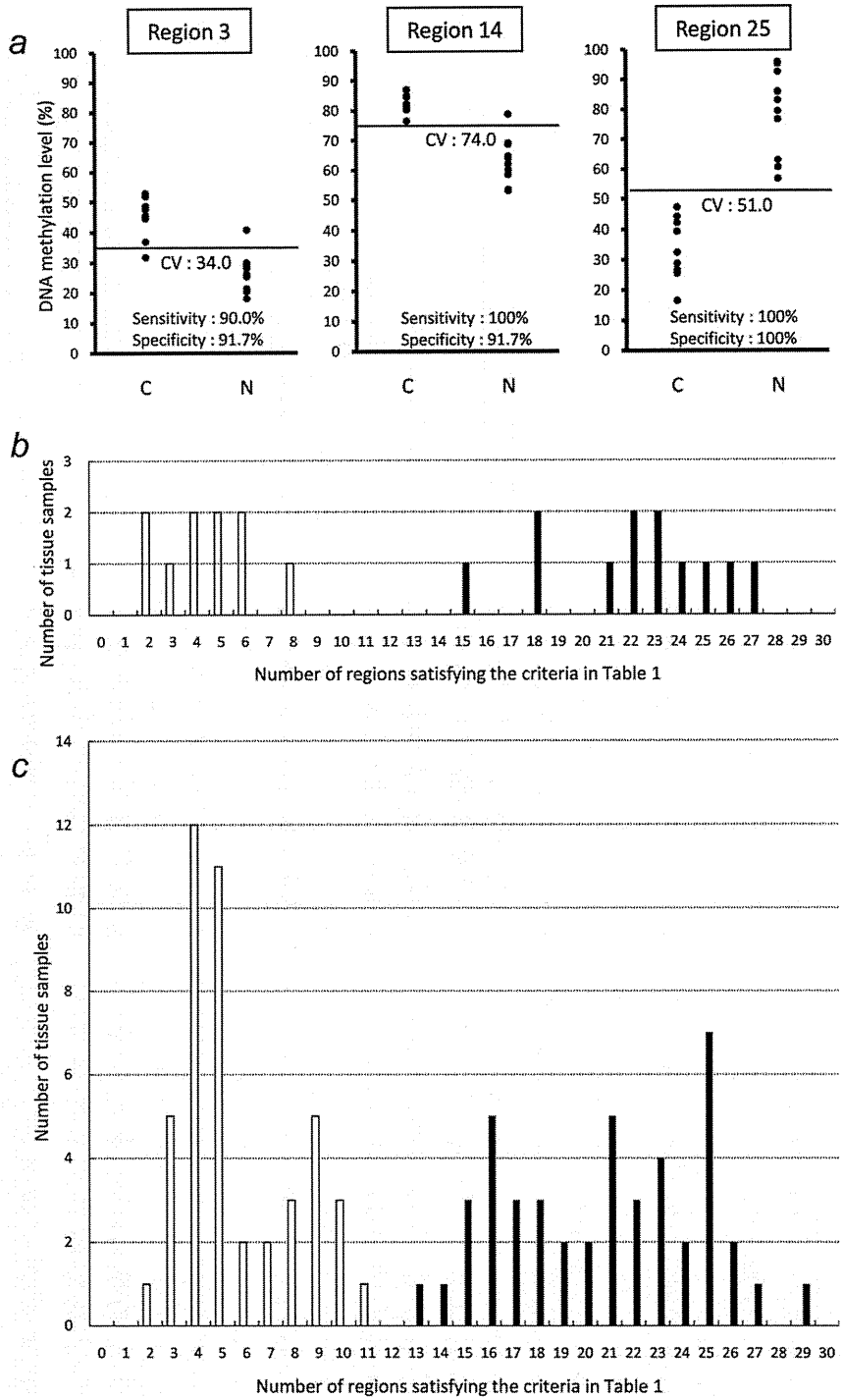

Figure 3. The criteria for carcinogenetic risk estimation based on pyrosequencing. (*a*) Scattergrams of DNA methylation levels in samples of normal liver tissue (C1–C10) and samples of noncancerous liver tissue obtained from patients with HCCs (N1–N12) in the learning cohort for representative regions. Using the cutoff values (CV, %) described in each panel, N-samples in the learning cohort were discriminated from C-samples with sufficient sensitivity and specificity. (*b*) Histogram showing the number of regions satisfying the criteria described in Table 1 in samples C1–C10 (clear columns) and N1–N12 (filled columns). On the basis of this histogram, we judged that when the noncancerous liver tissue satisfied the criteria in Table 1 for 15 or more than 15 regions, it was at high risk of carcinogenesis. (*c*) Validation of the criteria in Table 1 using an additional 90 samples of liver tissue in the validation cohort. All 43 validation samples satisfying the Table 1 criteria for 15 or more regions were N-samples (N13–N36, N38–N41 and N43–N57, filled columns), and 45 of 47 validation samples satisfying the Table 1 criteria for less than 15 regions were C-samples (C11–C55, clear columns). DNA methylation statuses for the 30 regions of N-samples and those of C-samples were completely mutually exclusive in the validation cohort.

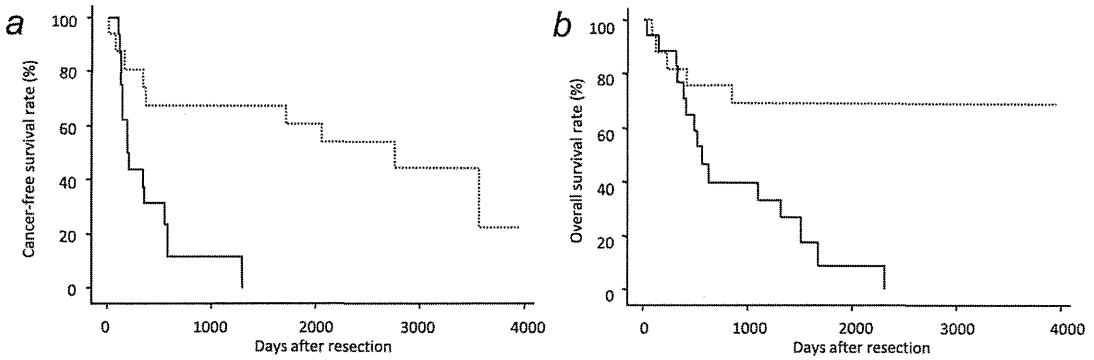

Figure 4. Correlation between DNA methylation status at the precancerous stage and patient outcome. Kaplan–Meier survival curves of patients with HCCs from whom samples N1–N34 were obtained. The cancer-free (*a*; $p = 0.0023$) and overall (*b*; $p = 0.0015$) survival rates of patients with HCCs satisfying the criteria in Table 1 for 23 (the median of the number of regions satisfying the Table 1 criteria) or more than 23 regions in their samples of noncancerous liver tissue ($n = 17$, solid lines) were significantly lower than those of patients with HCCs satisfying the criteria in Table 1 for less than 23 regions ($n = 17$, broken lines).

HCCs in the learning cohort was discriminated from normal liver tissue with sufficient sensitivity and specificity (Fig. 3*a*). On the remaining 45 CpG sites, such discrimination was performed with a sensitivity or specificity of 70% or more than 70%. If several CpG sites were measured using one sequencing primer, one cutoff value was set for the region covered by the sequencing primer using the average DNA methylation levels of the several CpG sites. Then the 30 cutoff values were set for 30 regions including the 45 CpG sites, and their sensitivity and specificity are shown in Table 1. Chromosomal loci and characteristics of the 30 regions (CpG islands or not, exons or introns of specific genes or noncoding regions) are also summarized in Table 1.

A histogram showing the number of regions satisfying the criteria listed in Table 1 for samples C1–C10 and N1–N12 in the learning cohort is shown in Figure 3*b*. On the basis of Figure 3*b*, we finally established that when liver tissue satisfied the criteria in Table 1 for 15 or more regions, it was judged to be at high risk of carcinogenesis. Based on this definition both the sensitivity and specificity for diagnosis of noncancerous liver tissue obtained from patients with HCCs in the learning cohort as being at high risk of carcinogenesis were 100%.

To confirm these criteria, an additional 90 samples of liver tissue were analyzed by pyrosequencing as a validation study (Fig. 3*c*). All of the 43 validation samples satisfying the criteria in Table 1 for 15 or more regions were noncancerous liver tissue obtained from patients with HCCs (N13–N36, N38–N41 and N43–N57), and 45 of the 47 validation samples satisfying the Table 1 criteria for less than 15 regions were normal liver tissue (C11–C55). DNA methylation statuses for the 30 regions of noncancerous liver tissue samples from patients with HCCs and those of normal liver tissue samples were completely mutually exclusive in the validation cohort (Fig. 3*c*), and our criteria enabled diagnosis of noncancerous liver tissue from patients with HCCs in the validation cohort as being at high risk of carcinogenesis with 95.6% sensitivity and 100% specificity.

Clinicopathological significance of DNA methylation status in the 30 regions

To estimate the clinicopathological significance of DNA methylation status in the 30 regions, 34 samples of noncancerous liver tissue from patients with HCCs (N1–N34) in both the learning and validation cohorts for whom follow-up data had been obtained were divided into two groups according to the number of regions satisfying the criteria (≥23 [the median of the number of regions satisfying the Table 1 criteria] regions *vs.* <23 regions). The period covered ranged from 11 to 3,936 days (mean: 1,417 days). The cancer-free and overall survival rates for patients with HCCs satisfying the criteria in Table 1 for 23 or more regions in their noncancerous liver tissue were significantly lower than those of patients with HCCs satisfying the Table 1 criteria for less than 23 regions (Fig. 4, $p = 0.0023$ and $p = 0.0015$, respectively). These data suggested that clinicopathologically valid DNA methylation alterations associated with patient outcome are already present at the precancerous stage.

With respect to all 57 samples of noncancerous liver tissue (N1–N57), the difference in the number of regions satisfying the criteria listed in Table 1 between liver tissue samples showing chronic hepatitis ($n = 26$, 19.6 ± 3.7) and those showing cirrhosis ($n = 31$, 22.0 ± 3.9) was marginal ($p = 0.0206$). For comparison, the DNA methylation levels of 30 regions in 14 additional liver tissue samples (V1–V14) obtained from patients who were infected with HBV or HCV, but who had never developed HCCs, were analyzed by pyrosequencing. The average number of regions satisfying the

Int. J. Cancer: **129**, 1170–1179 (2011) © 2011 UICC

Table 1 criteria was significantly lower in V1–V14 (12.0 ± 5.0), than in N1–N57 (20.9 ± 4.0, $p < 0.0001$). These data suggested that our criteria do not simply reflect the presence of hepatitis virus infection, inflammation or fibrosis at the chronic hepatitis and liver cirrhosis stages, but in fact reflect the carcinogenetic risk itself.

Discussion

For appropriate surveillance of patients at the precancerous stage for HCCs, the criteria for carcinogenetic risk estimation should be explored. As considerable numbers of liver tissue samples obtained from patients with HBV or HCV infection indicate a future risk of HCCs, even if HCCs are not yet present, comparison between liver tissue samples obtained from patients with HBV or HCV infection but without HCCs and those obtained from patients with HBV or HCV infection but also showing HCCs, is not an adequate strategy for establishing criteria for carcinogenetic risk estimation. Therefore, in our previous study, we focused on BAC clones whose signal ratios differed significantly between samples of normal liver tissue obtained from patients without HBV or HCV infection and samples of noncancerous liver tissue obtained from patients with HCCs (namely BAC clones on which DNA methylation alterations had occurred at the precancerous stage), and also those on which such DNA methylation alterations had been inherited by HCCs themselves from precancerous conditions. In this way, we successfully established such criteria using BAC array-based methods.[18]

In our study, the reliability of BAMCA was again confirmed: BAMCA was able to provide an overview of DNA methylation tendency in large regions of chromosomes, and especially was able to detect DNA methylation alterations occurring in a coordinated manner in the entire BAC region. However, the exact CpG sites that are of diagnostic impact are unclear, because several *Xma* I/*Sma* I sites that are effective in BAMCA generally exist on each of the BAC clones with an average insert size of 170 kbp.[20] Moreover, as BAMCA requires a large amount of genomic DNA, and the technique is somewhat cumbersome, our previous criteria based on BAMCA may not be suitable for clinical uses such as risk estimation based on liver biopsy specimens. Therefore, we employed Pyrosequencing™ technology, which is an excellent tool for quantitative estimation of DNA methylation levels at specific CpG sites.

Although numerous *Xma* I/*Sma* I sites are located within CpG islands, one or two *Xma* I/*Sma* I sites on each CpG island were analyzed because of difficulties with the design of the PCR and sequencing primers. Then, DNA methylation levels at 203 CpG sites on the 25 BAC clones that comprised our previous criteria based on BAMCA were evaluated quantitatively by pyrosequencing. By combining the 30 regions including 45 specific CpG sites, which were revealed to have a large diagnostic impact, the specificity of the criteria for carcinogenetic risk estimation was successfully improved in comparison with our previous criteria based on BAMCA[18]: the sensitivity and specificity of the criteria after revision by pyrosequencing were both 100% in the learning cohort and were 95.6% and 100% in the validation cohort, respectively.

Only one region (region 20 in Table 1) among 30 regions that had been used for defining the revised criteria for carcinogenetic risk estimation was located within the promoter region of a specific gene (general receptor for phosphoinositides 1-associated scaffold protein), although DNA methylation alterations in promoter regions are known to be one of most consistent epigenetic changes in human cancers.[24] At the risk stage, but not in established cancers, it is feasible that DNA methylation alterations do not expand immediately to the promoter regions of specific genes, such as tumor-related genes. However, 20, 19 and 9 regions that had been used for defining the revised criteria were located within gene bodies, non-CpG islands, and noncoding regions, respectively, which have been overlooked as targets of DNA methylation alterations during multistage human carcinogenesis. Although most of the recently developed detection technologies, such as promoter arrays and CpG island arrays, are sequence-based methods and cannot comprehensively measure the DNA methylation status of gene bodies, non-CpG islands and noncoding regions,[25,26] our findings indicate that meticulous examination of such sequences is also important for establishment of optimal diagnostic indicators.

DNA methylation status in the 30 regions in noncancerous liver tissue at the precancerous stage was significantly correlated with both cancer-free and overall survival rates of patients with HCCs (Fig. 4). Although prognostication before development of HCCs was not a clinically relevant issue, and we never intended to perform such prognostication, we can consider that DNA methylation alterations determining patient outcome had already accumulated at the precancerous stage, based on the data in Figure 4. As DNA methylation status is not randomly altered at the precancerous stage, and DNA methylation profiles in noncancerous liver tissue have been proven to be clinicopathologically valid, it is feasible that such profiles could be optimal indicators for carcinogenetic risk estimation.

The difference in the number of regions satisfying the criteria listed in Table 1 between liver tissue samples showing chronic hepatitis and those showing cirrhosis was marginal, indicating that our criteria were not simply associated with inflammation or fibrosis. In addition, the average number of regions satisfying the Table 1 criteria were significantly lower in liver tissue from patients without HCCs (V1–V14) than in noncancerous liver tissue from patients with HCCs (N1–N34), even though the patients from whom V1–V14 were obtained were infected with HBV or HCV. DNA methylation status in the 30 regions does not depend on hepatitis virus infection but may actually reflect the carcinogenetic risk itself. Therefore, our criteria not only discriminate noncancerous liver tissue from patients with HCCs from normal liver tissues but also may be applicable for classifying liver tissue obtained from patients who are being followed up

because of HBV or HCV infections, chronic hepatitis or cirrhosis into that which may generate HCCs and that which will not.

During surveillance at the precancerous stage, to reveal the baseline liver histology, microscopic examination of liver biopsy specimens is performed in patients with HBV or HCV infection before interferon therapy.[27,28] Therefore, carcinogenetic risk estimation using such liver biopsy specimens will be advantageous for close follow-up of patients who are at high risk of HCC development. We have confirmed that pyrosequencing can be performed using a very small amount of degraded DNA extracted from formalin-fixed and paraffin-embedded liver biopsy specimens (unpublished data). We now intend to prospectively validate the reliability of risk estimation based on the revised criteria using pyrosequencing in liver biopsy specimens obtained before interferon therapy from a large cohort of patients with HBV or HCV infection.

Acknowledgements

Author R.N. received a Research Resident Fellowship from the Foundation for Promotion of Cancer Research in Japan.

References

1. Chang MH, Chen CJ, Lai MS, Hsu HM, Wu TC, Kong MS, Liang DC, Shau WY, Chen DS. Universal hepatitis B vaccination in Taiwan and the incidence of hepatocellular carcinoma in children. Taiwan Childhood Hepatoma Study Group. *N Engl J Med* 1997;336:1855–9.
2. Tanaka Y, Hanada K, Mizokami M, Yeo AE, Shih JW, Gojobori T, Alter HJ. Inaugural article: a comparison of the molecular clock of hepatitis C virus in the United States and Japan predicts that hepatocellular carcinoma incidence in the United States will increase over the next two decades. *Proc Natl Acad Sci USA* 2002; 99:15584–9.
3. Jones PA, Baylin SB. The epigenomics of cancer. *Cell* 2007;128:683–92.
4. Sharma S, Kelly TK, Jones PA. Epigenetics in Cancer. *Carcinogenesis* 2009;31:27–36.
5. Kanai Y, Hirohashi S. Alterations of DNA methylation associated with abnormalities of DNA methyltransferases in human cancers during transition from a precancerous to a malignant state. *Carcinogenesis* 2007;28:2434–42.
6. Kanai Y. Alterations of DNA methylation and clinicopathological diversity of human cancers. *Pathol Int* 2008;58:544–58.
7. Kanai Y, Ushijima S, Tsuda H, Sakamoto M, Sugimura T, Hirohashi S. Aberrant DNA methylation on chromosome 16 is an early event in hepatocarcinogenesis. *Jpn J Cancer Res* 1996;87:1210–7.
8. Kondo Y, Kanai Y, Sakamoto M, Mizokami M, Ueda R, Hirohashi S. Genetic instability and aberrant DNA methylation in chronic hepatitis and cirrhosis—a comprehensive study of loss of heterozygosity and microsatellite instability at 39 loci and DNA hypermethylation on 8 CpG islands in microdissected specimens from patients with hepatocellular carcinoma. *Hepatology* 2000;32:970–9.
9. Kaneto H, Sasaki S, Yamamoto H, Itoh F, Toyota M, Suzuki H, Ozeki I, Iwata N, Ohmura T, Satoh T, Karino Y, Satoh T, et al. Detection of hypermethylation of the p16(INK4A) gene promoter in chronic hepatitis and cirrhosis associated with hepatitis B or C virus. *Gut* 2001; 48:372–7.
10. Saito Y, Kanai Y, Sakamoto M, Saito H, Ishii H, Hirohashi S. Overexpression of a splice variant of DNA methyltransferase 3b. DNMT3b4, associated with DNA hypomethylation on pericentromeric satellite regions during human hepatocarcinogenesis. *Proc Natl Acad Sci USA* 2002;99:10060–5.
11. Saito Y, Kanai Y, Nakagawa T, Sakamoto M, Saito H, Ishii H, Hirohashi S. Increased protein expression of DNA methyltransferase (DNMT) 1 is significantly correlated with the malignant potential and poor prognosis of human hepatocellular carcinomas. *Int J Cancer* 2003;105:527–32.
12. Kanai Y. Genome-wide DNA methylation profiles in precancerous conditions and cancers. *Cancer Sci* 2009;101:36–45.
13. Arai E, Kanai Y. DNA methylation profiles in precancerous tissue and cancers: carcinogenetic risk estimation and prognostication based on DNA methylation status. *Epigenomics* 2010;2: 467–81.
14. Misawa A, Inoue J, Sugino Y, Hosoi H, Sugimoto T, Hosoda F, Ohki M, Imoto I, Inazawa J. Methylation-associated silencing of the nuclear receptor 1I2 gene in advanced-type neuroblastomas, identified by bacterial artificial chromosome array-based methylated CpG island amplification. *Cancer Res* 2005;65:10233–42.
15. Sugino Y, Misawa A, Inoue J, Kitagawa M, Hosoi H, Sugimoto T, Imoto I, Inazawa J. Epigenetic silencing of prostaglandin E receptor 2 (PTGER2) is associated with progression of neuroblastomas. *Oncogene* 2007;26:7401–13.
16. Tanaka K, Imoto I, Inoue J, Kozaki K, Tsuda H, Shimada Y, Aiko S, Yoshizumi Y, Iwai T, Kawano T, Inazawa J. Frequent methylation-associated silencing of a candidate tumor-suppressor, CRABP1, in esophageal squamous-cell carcinoma. *Oncogene* 2007;26:6456–68.
17. Arai E, Ushijima S, Fujimoto H, Hosoda F, Shibata T, Kondo T, Yokoi S, Imoto I, Inazawa J, Hirohashi S, Kanai Y. Genome-wide DNA methylation profiles in both precancerous conditions and clear cell renal cell carcinomas are correlated with malignant potential and patient outcome. *Carcinogenesis* 2009;30:214–21.
18. Arai E, Ushijima S, Gotoh M, Ojima H, Kosuge T, Hosoda F, Shibata T, Kondo Y, Yokoi S, Imoto I, Inazawa J, Hirohashi S, et al. Genome-wide DNA methylation profiles in liver tissue at the precancerous stage and in hepatocellular carcinoma. *Int J Cancer* 2009;125:2854–62.
19. Nishiyama N, Arai E, Chihara Y, Fujimoto H, Hosoda F, Shibata T, Kondo T, Tsukamoto T, Yokoi S, Imoto I, Inazawa J, Hirohashi S, et al. Genome-wide DNA methylation profiles in urothelial carcinomas and urothelia at the precancerous stage. *Cancer Sci* 2010;101: 231–40.
20. Osoegawa K, Mammoser AG, Wu C, Frengen E, Zeng C, Catanese JJ, de Jong PJ. A bacterial artificial chromosome library for sequencing the complete human genome. *Genome Res* 2001;11: 483–96.
21. Clark SJ, Harrison J, Paul CL, Frommer M. High sensitivity mapping of methylated cytosines. *Nucleic Acids Res* 1994;22: 2990–7.
22. Shen L, Guo Y, Chen X, Ahmed S, Issa JP. Optimizing annealing temperature overcomes bias in bisulfite PCR methylation analysis. *Bio Techniques* 2007; 42:48–58.
23. Gao W, Kondo Y, Shen L, Shimizu Y, Sano T, Yamao K, Natsume A, Goto Y, Ito M, Murakami H, Osada H, Zhang J, et al. Variable DNA methylation patterns associated with progression of disease in hepatocellular carcinomas. *Carcinogenesis* 2008;29:1901–10.
24. Baylin SB, Ohm JE. Epigenetic gene silencing in cancer—a mechanism for early oncogenic pathway addiction? *Nat Rev Cancer* 2006;6:107–16.

25. Estecio MR, Issa JP. Tackling the methylome: recent methodological advances in genome-wide methylation profiling. *Genome Med* 2009;1:106.
26. Mohn F, Schubeler D. Genetics and epigenetics: stability and plasticity during cellular differentiation. *Trends Genet* 2009; 25:129–36.
27. Arase Y, Ikeda K, Suzuki F, Suzuki Y, Kobayashi M, Akuta N, Hosaka T, Sezaki H, Yatsuji H, Kawamura Y, Kobayashi M, Kumada H. Comparison of interferon and lamivudine treatment in Japanese patients with HBeAg positive chronic hepatitis B. *J Med Virol* 2007;79: 1286–92.
28. Yoshida H, Tateishi R, Arakawa Y, Sata M, Fujiyama S, Nishiguchi S, Ishibashi H, Yamada G, Yokosuka O, Shiratori Y, Omata M. Benefit of interferon therapy in hepatocellular carcinoma prevention for individual patients with chronic hepatitis C. *Gut* 2004;53: 425–30.

Proteomic Profiling Reveals the Prognostic Value of Adenomatous Polyposis Coli–End-Binding Protein 1 in Hepatocellular Carcinoma

Tatsuya Orimo,[1,5] Hidenori Ojima,[2] Nobuyoshi Hiraoka,[2] Shigeru Saito,[1,4] Tomoo Kosuge,[3] Tatsuhiko Kakisaka,[5] Hideki Yokoo,[5] Kazuaki Nakanishi,[5] Toshiya Kamiyama,[5] Satoru Todo,[5] Setsuo Hirohashi,[1] and Tadashi Kondo[1]

Histological differentiation is a major pathological parameter associated with poor prognosis in patients with hepatocellular carcinoma (HCC) and the molecular signature underlying HCC differentiation may involve key proteins potentially affecting the malignant characters of HCC. To develop prognostic biomarkers for HCC, we examined the global protein expression profiles of 45 surgically resected tissues, including 27 HCCs with different degree of histological differentiation, 11 adjacent nontumor tissues, and seven normal liver tissues. Unsupervised classification grouped the 45 samples according to their histological classification based on the protein expression profiles created by laser microdissection and two-dimensional difference gel electrophoresis (2D-DIGE). Statistical analysis and mass spectrometry identified 26 proteins with differential expression, of which 14 were functionally linked to c-Myc, AP-1, HIF1A, hepatocyte nuclear factor 4 alpha, or the Ras superfamily (RhoA, CDC42, and Rac1). Among the proteins identified, we focused on APC-binding protein EB1 (EB1) because it was dominantly expressed in poorly differentiated HCCs, which generally correlate with the poor prognosis in patients with HCC. In addition, EB1 is controlled by c-Myc, RhoA, and CDC42, which have all been linked to HCC malignancy. Immunohistochemistry in a further 145 HCC cases revealed that EB1 significantly correlated with the degree of histological differentiation ($P < 0.001$), and univariate and multivariate analyses indicated that EB1 is an independent prognostic factor for recurrence (hazard ratio, 2.740; 95% confidence interval, 1.771-4.239; $P < 0.001$) and survival (hazard ratio, 2.256; 95% confidence interval, 1.337-3.807; $P = 0.002$) of patients with HCC after curative surgery. *Conclusion*: Proteomic profiling revealed the molecular signature behind the progression of HCC, and the prognostic value of EB1 in HCC. (HEPATOLOGY 2008;48:1851-1863.)

Hepatocellular carcinoma (HCC) is one of the most common and aggressive malignancies world-wide and is the third leading cause of cancer death.[1] HCC is a major health problem with high prevalence in Asia and Africa,[2,3] and recent studies indicated that the incidence of HCC has increased substantially in the United States and the United Kingdom over the last decades.[4,5] The prognosis for patients with HCC

Abbreviations: 2D-DIGE, two-dimensional difference gel electrophoresis; AP-1, activator protein 1; APC, adenomatous polyposis coli; C/EBP beta, CCAAT/enhancer-binding protein, beta subunit; CSA, catalyzed signal amplification; Cy, cyanine; EB1, APC-binding protein EB1; HCC, hepatocellular carcinoma; HIF1A, hypoxia-inducible factor 1, alpha subunit; mDia2, mammalian Diaphanous-related formin; PAGE, polyacrylamide gel electrophoresis; Rac, ras-related C3 botulinum toxin substrate, Ras, ras sarcoma oncoprotein; RhoA, ras homology gene family, member A; SDS, sodium dodecyl sulfate; TNM, tumor-node-metastasis; XML, extensible markup language.

From the [1]Proteome Bioinformatics Project; [2]Pathology Division; [3]Division of Hepatobiliary and Pancreatic Surgery, National Cancer Center Hospital, Tokyo, Japan; [4]Chemistry and Bioinformatics Department, Infocom Corporation, Tokyo, Japan; and [5]Department of General Surgery, Hokkaido University Graduate School of Medicine, Sapporo, Japan.

Received March 26, 2008; accepted July 21, 2008.

Supported by the Ministry of Health, Labor and Welfare, and by the Program for Promotion of Fundamental Studies in Health Sciences of the Organization for Pharmaceutical Safety and Research of Japan. T.O. is a Research Resident Fellowships awardee from the Foundation for Promotion of Cancer Research in Japan.

Address reprint requests to: Tadashi Kondo, M.D., Ph.D., Proteome Bioinformatics Project, National Cancer Center Research Institute, 5-1-1 Tsukiji, Chuo-ku, Tokyo 104-0045, Japan. E-mail: takondo@ncc.go.jp; fax: 81-3-3547-5298.

Published online in Wiley InterScience (www.interscience.wiley.com).

DOI 10.1002/hep.22552

Potential conflict of interest: Nothing to report.

Additional Supporting Information may be found in the online version of this article.

Table 1. A List of Identified Proteins

Accession No.*	Identified Protein*	Locus†	Spot No.†	*P* Value*	pI (cal)‖	MW (cal) (D)‖	Protein Score¶	Peptide Matches	Sequence Coverage (%)
Proteins in cluster A**									
Function									
Cell proliferation									
P12004	Proliferating cell nuclear antigen	20pter-p12	2794	1.93E-03	4.57	29092	94	2	10
			2800	4.65E-03	4.57	29092	189	2	10
			2892	3.04E-03	4.57	29092	245	4	16.1
Q15691	APC-binding protein EB1	20q11.1-q11.23	3360	7.64E-03	5.02	30020	189	4	20.6
P51858	Hepatoma-derived growth factor	lq21-q23	2938	4.54E-03	4.7	26886	200	4	21.7
Protein folding									
P14625	Heat shock protein 90 kDa beta member 1	12q24.2-q24.3	1696	2.89E-03	4.76	92696	267	5	6.5
			1741	1.25E-03	4.76	92696	717	23	17.6
Q9UHV9	Prefoldin subunit 2	1q23.3	4730	5.86E-03	6.2	16695	186	3	22.7
Cytoskeletal/structural protein									
P20700	Lamin-B1	5q23.3-q31.1	1080	3.73E-03	5.11	66522	821	19	27.9
P08670	Vimentin	10p13	1968	5.91E-03	5.06	53545	797	20	32.7
Signal transduction									
P06702	Protein S100-A9	1q21	4680	5.02E-03	5.71	13291	81	2	26.3
Transport									
P61923	Customer subunit zeta-1	12q13.2-q13.3	4530	8.44E-03	4.69	20242	117	2	11.9
Proteins in cluster B**									
Amino acid metabolism									
O95954	Formimidoyltransferase-cyclodeaminase	21q22.3	1398	5.07E-03	5.58	59574	422	7	17.7
			1417	1.04E-03	5.58	59574	483	9	17.6
			1422	1.19E-03	5.58	59574	482	9	19.4
Q00266	S-pdenosylmethionlne synthetase isoform type-1	10q22	2004	1.26E-03	5.86	44190	124	2	8.4
P16930	Fumarylacetoacetase	15q23-q25	2110	2.62E-03	6.46	46743	214	4	9.3
P05089	Arginase-1	6q23	2630	1.67E-03	6.72	34884	274	6	17.7
Q14749	Glycine N-methyltransferase	6p12	2696	7.85E-03	6.58	33046	158	3	14.3
Oxidoreduction									
P32754	4-hydroxyphenylpyruvate dioxygenase	12q24-qter	2376	7.33E-03	6.5	44946	539	10	25.5
			2385	6.83E-03	6.5	44946	734	18	37
NP_036335	Glyoxylate reductase/hydroxypyruvate reductase	9q12	2520	9.29E-03	7.01	36045	312	6	19.5
			2527	2.06E-03	7.01	36045	122	3	8.2
O95154	Aflatoxin B1 aldehyde reductase member 3	1p35.1-p36.23	2884	5.26E-03	6.67	37582	412	6	23.6
P78417	Glutathione transferase omega-1	10q25.1	3824	2.73E-03	6.23	27833	202	4	18.3
Lipid metabolism									
P54868	Hydroxymethylglutaryl-CoA synthase, mitochondrial precursor	1p13-p12	1709	1.60E-03	8.4	57113	174	3	6.5
P45954	Short/branched chain specific acyl-CoA dehydrogenase, mitochondrial precursor	10q26.13	2428	8.62E-03	6.53	47797	469	8	21.8
P16219	Short-chain specific acyl-CoA dehydrogenase, mitochondrial precursor	12q22-qter	2526	1.01E-03	8.13	44611	683	16	35.7
			2542	2.69E-03	8.13	44611	376	8	17.7
P30084	Enoyl-CoA hydratase, mitochondrial precursor	10q26.2-q26.3	3294	7.45E-03	8.34	31823	242	3	16.9

Table 1. (Continued)

Accession No.*	Identified Protein*	Locus†	Spot No.†	*P* Value*	pI (cal)‖	MW (cal) (D)‖	Protein Score¶	Peptide Matches	Sequence Coverage (%)
			3304	8.65E-03	8.34	31823	116	2	9.7
			3332	8.74E-03	8.34	31823	205	6	16.9
			3338	8.69E-03	8.34	31823	529	12	31.7
			3378	8.67E-03	8.34	31823	287	5	20
			3402	6.06E-03	8.34	31823	308	5	22.8
			3420	4.11E-03	8.34	31823	290	8	20
			3465	4.17E-03	8.34	31823	473	8	31.4
Chycometabolism									
P05062	Fructose-bisphosphate aldolase B	9q21.3-q22.2	2187	5.79E-03	8	39961	195	3	9.6
P09467	Fructose-1,6-bisphosphatase 1	9q22.3	2661	8.97E-03	6.6	37059	486	11	36.5
Signal transduction									
P52566	Rho GDP-dissociation Inhibitor 2	12p12.3	4046	1.49E-03	5.1	22900	136	2	15
Isomerization									
P30039	MAWD-binding protein	10pter-q25.3	3284	5.68E-03	6.06	32050	118	2	8.7

*Proteins in Supporting Fig. 3 are shown as bold.

*Accession numbers of proteins and protein name were derived from Swiss-Prot and NCBI nonredundant databases.

Protein function was categorized by accessing Gene Ontology database (http://www.geneontology.org/) and literature curation.

†Gene locus was determined according to NCBI database.

‡Spot numbers refer to those in Figure 2C and Supplemental Fig. 1.

§Bonferroni adjusted *P* value.

‖Theoretical isoelectric point and molecular weight obtained from Swiss-Prot and the ExPASy database (http://au.expasy.org).

¶Mascot score for the identified proteins based on the peptide ions score ($P < 0.05$) (http://www.matrixscience.com).

**Cluster A and B are shown in Fig. 2C.